Chapter 30
Pragmatic Design Methods Using Adaptive Controller Structures for Mechatronic Applications with Variable Parameters and Working Conditions

Stefan Preitl, Radu-Emil Precup, Zsuzsa Preitl, Alexandra-Iulia Stînean, Claudia-Adina Dragoş and Mircea-Bogdan Rădac

"*The PID controller can be said to be 'the bread and the butter' of the control engineering*".

(K.-J. Åström)

Abstract This chapter treats two pragmatic design methods for controllers dedicated to mechatronic applications working under variable conditions; for such applications adaptive structures of the control algorithms are of great interest. Basically, the design is based on two extensions of the modulus optimum method and of the symmetrical optimum method (SO-m): the Extended SO-m and the double parameterization of the SO-m (2p-SO-m). Both methods are introduced by the authors and they use PI(D) controllers that can ensure high control performance: increased value of the phase margins, improved tracking performance, and efficient

S. Preitl (✉) · R.-E. Precup · A.-I. Stînean · C.-A. Dragoş · M.-B. Rădac
Department of Automation and Applied Informatics, "Politehnica" University of Timisoara, Bd. V. Parvan 2, 300223 Timisoara, Romania
e-mail: stefan.preitl@aut.upt.ro

R.-E. Precup
e-mail: radu.precup@aut.upt.ro

A.-I. Stînean
e-mail: alexandra-iulia.stinean@aut.upt.ro

C.-A. Dragoş
e-mail: claudia.dragos@aut.upt.ro

M.-B. Rădac
e-mail: mircea.radac@aut.upt.ro

Z. Preitl
Siemens A.G., Erlangen, Germany
e-mail: zsuzsap@yahoo.com

G.M. Dimirovski (ed.), *Complex Systems*, Studies in Systems, Decision and Control 55, DOI 10.1007/978-3-319-28860-4_30

disturbance rejection. A short and systematic presentation of the methods and digital implementation aspects using an adaptive structure of the algorithms for industrial applications are given. The application deals with a cascade speed control structure for a driving system with continuously variable parameters, i.e., electrical drives with variable reference input, variable moment of inertia and variable disturbance input.

List of Abbreviations

SO-m	Symmetrical Optimum method
Mo-M	Modulus Optimum method
ESO-m	Extended Symmetrical Optimum method
2p-SO-m	Double parameterization of the SO-m
2-DOF	Two Degree of Freedom
VMI	Variable Moment of Inertia
t.f.	Transfer function
c.a.	Control algorithm
C-VR-MI-LD	Continuously Variable Reference, Moment of Inertia and Load Disturbance
DC-m, BLDC-m	DC-motors, Brush-Less DC-motors
MM	Mathematical Model
CS	Control Structure
CCS	Cascade Control Structure

30.1 Introduction: The Design Methods

The basic ideas of frequency domain optimization—based on the modulus optimum conditions—are synthesized in [1, 2] as:

$$M_r(\omega) = |H_r(j\omega)| \approx 1 \text{ , for values of } \omega \geq 0 \text{ as large as possible} \tag{30.1.1}$$

$$M_{v1,v2}(\omega) = |H_{v1,v2}(j\omega)| \approx 0 \text{ for values of } \omega \geq 0 \text{ as large as possible.} \tag{30.1.2}$$

Decomposing the expressions of $M_r(\omega)$, $M_{v1}(\omega)$, $M_{v2}(\omega)$ into Mc-Laurin series, the design conditions can be derived on the basis of the following requirements:

$$M_r(0) = 1, \left.\frac{d^{\nu}|M_r(\omega)|}{d\omega^{\nu}}\right|_{\omega=0} = 0 \quad \text{(a)} \tag{30.1.3}$$

$$M_{v1,v2}(0) = 0, \left.\frac{d^{\nu}|M_{v1,v2}(\omega)|}{d\omega^{\nu}}\right|_{\omega=0} = 0 \quad \text{(b)} \tag{30.1.4}$$

They are called modulus optimum (MO) conditions. Considering the classical control structure given in Fig. 30.1, the basic relations (neglecting the measurement noise) are expressed as

$$y(s) = H_0(s)S(s)r(s) + S(s)v_1(s) + P(s)S(s)v_2(s) \text{ and } H_0(s) = C(s) \cdot P(s) \tag{30.1.5}$$

$$u(s) = C(s)S(s)r(s) - C(s)S(s)v_1(s) - H_0(s)S(s)v_2(s), \tag{30.1.6}$$

$$\varepsilon(s) = S(s)r(s) - S(s)v_1(s) - P(s)S(s)v_2(s) \text{ and } r(s) = F(s)r_0(s) \tag{30.1.7}$$

$$S(s) = \frac{1}{1 + C(s) \cdot P(s)}, \; T(s) = \frac{C(s) \cdot P(s)}{1 + C(s) \cdot P(s)}, \; S(s) + T(s) = 1 \tag{30.1.8}$$

where $H_r(s)$, $H_{v1}(s)$ $H_{v2}(s)$, $H_0(s)$, $S(s)$, $T(s)$ are the main transfer functions (t.f. s) and characteristic functions of the system.

Many design methods based on the modulus optimum method (MO-m) and symmetrical optimum method (SO-m) conditions have been developed in various variants. Such examples include the basic approach due to Kessler [3, 4] and other ones developed afterwards and reported in [5–14].

The MO-m is applied in two classical variants:

- The first variant is based on determining domains of variation of controller parameters that satisfy the imposed requirements, finally determining "the best solution". This variant requires huge amount of calculation.
- The second variant is based on direct tuning relations. Applying this variant is closer to engineering practice.

This chapter treats two extensions related to the second variant, introduced by the authors in [6, 9] and focused on obtaining better dynamics of the control structure, enhancement of robustness, and enlarging of area of applications. The efficiency of controller tuning methods—regarding the basic variant but other tuning methods as well—can be proved in the time domain and in the frequency domain. The methods found various extensions in fuzzy control and so on, and they are currently used in several applications.

This chapter is structured as follows. In Sect. 30.2 a short overview of MO-m and SO-m in their practical version is synthesized. Section 30.3 is focused on two pragmatic extensions of SO-m (proposed by the authors); the local conclusions are

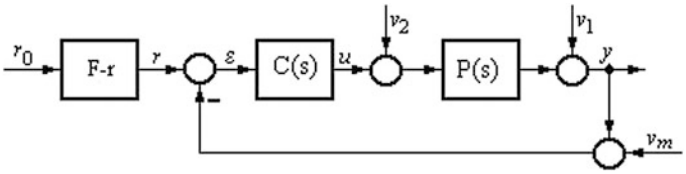

Fig. 30.1 Basic structure of the control loop

focused on versatility of the design, and its applicability for systems with plants characterized by variable parameters. Some possibilities to enhance the basic performances are given. Implementation in the form of a variable structure controller with bumpless transfer of the control signal is given. Section 30.4 offers an application example for systems with variable parameters: a control structure (CS) for a mechatronic system with variable parameters, the control solution for a winding system. Detailed analysis of the performances—including sensitivity analysis aspects—and the versatility of the solution prove its applicability. Section 30.5 is dedicated to some concluding remarks.

30.2 Pragmatic Forms of the Modulus Optimum Method and of the Symmetrical Optimum Method

The MO-m and the SO-m are dedicated mainly to servo systems [1–4] where they prove to be efficient [15]. Both methods are characterized by the fact that in the open-loop t.f. $H_0(s)$ (30.1.5), the result is a single (in case of MO-m) or a double pole (in case of SO-m) in origin and the parameters of the controllers (PI(D)-type) can be computed—and, if it is necessary, recalculated online—by means of compact formulas.

Basically, the MO-m and the SO-m design situations correspond to benchmark-type model for the plant and typical controllers—of PI(D) type—eventually, extended with lag components (L) and—in extension—with reference filters; they are synthesized in Table 30.1—for MO-m—and Table 30.2—for SO-m (T_Σ includes the effects of small time constants of the plant).

Mainly, the SO-m [1–4] is applicable—with some restrictions due to the resulting small phase reserve—to plants having a pole in origin (the main case for the positioning systems) characterized by a t.f. expressed in Table 30.2 for S0-1 and SO-2, when the use of a PI or a PID controller (having the t.f. expressed in Table 30.2 for S0-1 and SO-2; in this last case the pole-zero cancelation is applied $T_r' = T_1$).

k_p is the process gain, T_1 characterizes the mechanical time constant, T_2 and T_Σ characterize smaller time constants, having $T_1 \gg T_2 > T_\Sigma$

Table 30.1 The main design cases for MO-m (Kessler's variant)

Case	Plant, $P(s)$	Controller type $C(s)$	
0	1	2	3
MO-1.1 (a)	$\frac{k_p}{1+sT_\Sigma}$	I	$\frac{k_r}{s}$
MO-2.1 (b)	$\frac{k_p}{(1+sT_\Sigma)(1+sT_1)}$	PI	$\frac{k_r}{s}(1+sT_r)$, $T_r = T_1$
MO-3.1 (c)	$\frac{k_p}{(1+sT_\Sigma)(1+sT_1)(1+sT_2)}$ $T_1 > T_2 > T_\Sigma$	PID	$\frac{k_r}{s}(1+sT_r)(1+sT_r')$ $T_r = T_1$; $T_r' = T_2$

Table 30.2 The main design cases for SO-m (Kessler's variant)

Case	Plant, $P(s)$	Controller type $C(s)$	
0	1	2	3
SO-1 (a)	$\frac{k_p}{s(1+sT_\Sigma)}$	PI	$\frac{k_r}{s}(1+sT_r)$
SO-2 (b)	$\frac{k_p}{s(1+sT_\Sigma)(1+sT_1)}$ $T_\Sigma < 0.2T_1$	PID (-L1)	$\frac{k_r}{s}(1+sT_r)\left(1+sT_r'\right)$, $T_r' = T_1$ $\frac{k_r}{s}(1+sT_r)\frac{\left(1+sT_r'\right)}{(1+sT_f)}$ $T_r' = T_1$; $T_c'/T_f \approx (10 \ldots 20)$
SO-3 (c)	$\frac{k_p}{s(1+sT_\Sigma)(1+sT_1)(1+sT_2)}$ $T_1 > T_2 > T_\Sigma$, $T_\Sigma < 0.2T_1$	PID2-L2	$\frac{k_r}{s}(1+sT_r)\frac{\left(1+sT_r'\right)(1+sT_d)}{\left(1+sT_f'\right)(1+sT_f)}$ $T_r' = T_2$; $T_r'/T_f' \approx (10 \ldots 20)$ $T_d = T_2$; $T_d/T_f \approx (10 \ldots 20)$

Accordingly, the open-$H_0(s)$ and closed-loop t.f.s (with respect to the reference input r) $H_r(s)$ can be expressed as

$$H_0(s) = \frac{k_r k_p (1+sT_r)}{s^2(1+sT_\Sigma)},\ T_r > T_\Sigma.\ \text{and}\ H_r(s) = \frac{b_0 + b_1 s}{a_0 + a_1 s + a_2 s^2 + a_3 s^3}, \tag{30.2.1}$$

$(b_0 = a_0,\ b_1 = a_1,\ a_0 = k_r k_p,\ a_1 = k_r k_p T_r,\ a_2 = 1,\ a_3 = T_\Sigma)$ and the modulus

$$M_r(\omega) = |H_r(j\omega)| = \sqrt{\frac{a_0^2 + a_1^2\omega^2}{a_0^2 - (2a_0a_2 - a_1^2)\omega^2 - (2a_1a_3 - a_2^2)\omega^4 + a_3^2\omega^6}}. \tag{30.2.2}$$

The parameters of the "optimal controller" are obtained imposing in (30.2.2) the conditions

$$2a_0a_2 = a_1^2,\ 2a_1a_3 = a_2^2, \tag{30.2.3}$$

in the form of

$$k_c = \frac{1}{8k_P T_\Sigma^2},\ T_c = 4\,T_\Sigma\ (T_c' = T_1), \tag{30.2.4}$$

with $H_{r\,\text{opt}}(s)$ having $a_0 = 1,\ a_1 = 4T_\Sigma,\ a_2 = 8T_\Sigma^2,\ a_3 = 8T_\Sigma^3$, and $b_0 = 1,\ b_1 = 4T_\Sigma$. The "optimal performance" guaranteed by the SO-m—viz. $\sigma_1 \approx 43\,\%$ (overshoot), $t_s \approx 16.5T_\Sigma$ (settling time), $t_1 \approx 3.1T_\Sigma$ (first settling time) and a relatively small phase margin, $\phi_r \approx 36°$ (which is the main drawback of SO-m)—are seldom acceptable, Fig. 30.2. Mainly in cases of plants with variable parameters, the retuning of the controller is strongly recommended.

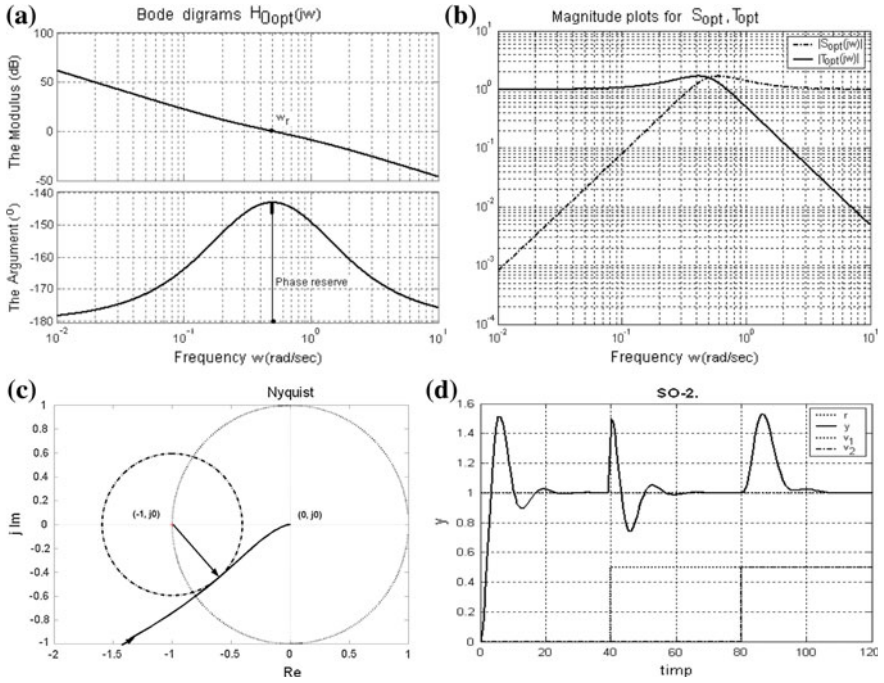

Fig. 30.2 The SO-m case: significant diagrams in frequency and time domain (for disturbance, only the case SO-1 is illustrated (*d*))

30.3 Extensions of the Symmetrical Optimum Method

Two efficient ways for performance enhancement—based on two extensions of the SO-m—have been introduced by the authors in [6, 9, 10], with focus on controller design based on benchmark-type models of the plant. They are synthesized as follows:

- the extended form of the symmetrical optimum method (ESO-m) [6], and
- the double parameterization form of the symmetrical optimum method (2p-SO-m) [9, 10].

Both methods employ the generalized form of Eq. (30.2.3)

$$\beta^{1/2} a_0 a_2 = a_1^2,\ \beta^{1/2} a_1 a_3 = a_2^2, \tag{30.3.1}$$

where β is the design parameter, whose value can be chosen by the designer, in correlation with desired performance indices. The methods are focused to fulfill an increased value for the phase margin, good (better) tracking performances, and efficient disturbance rejection.

30.3.1 The Extended Symmetrical Optimum Method (ESO-m)

The ESO-m [6, 16, 17] is dedicated mainly to controller tuning for positioning and tracking systems operating under continuously variable reference and plant parameters, characterized by the t.f.s in the forms given in Table 30.2(a)–(c). Applying the generalized form of the optimization relations (30.3.1), the compact parameter tuning equations are

$$k_c = \frac{1}{k_P \beta^{3/2} T_\Sigma^2}, \; T_c = \beta T_\Sigma \; (T_c' = T_1), \tag{30.3.2}$$

and as a result the characteristic t.f.s $H_0(s)$ and $H_r(s)$ will obtain the forms (30.3.3), which lead to significantly improved performance (see, for example, the phase margin characteristics).

$$H_0(s) = \frac{1 + \beta T_\Sigma s}{\beta^{3/2} T_\Sigma^2 s^2 (1 + T_\Sigma s)} \text{ and } H_r(s) = \frac{1 + \beta T_\Sigma s}{\beta^{3/2} T_\Sigma^3 s^3 + \beta^{3/2} T_\Sigma^2 s^2 + \beta T_\Sigma s + 1}. \tag{30.3.3}$$

Figure 30.3 offers the main control system performance indices as function of the design parameter β [6]; the recommended domain for β is $4 < \beta \leq 9\,(16)$. The main advantage is that the increase of the phase margin (accompanied with the decreasing of ω_c) also leads to increase of the settling time. The reference behaviors can be corrected using adequate reference filter F-r.

Extensive analyses of the method and experimental results are also presented also in [16] and [19]. Important supplementary aspects deal with:

- *Sensitivity function analysis.* Based on the relation of $S_0(s)$ the maximum sensitivity value M_{s0} and its inverse M_{S0}^{-1} can be calculated. Figure 30.4a–c illustrate the Nyquist diagrams calculated for $\beta = 4, 9, 16$; the $M_{S0} = f(\beta)$ circles and the values of M_{S0}^{-1} are also marked. The curves point out the increase of robustness when the value of β is increased.

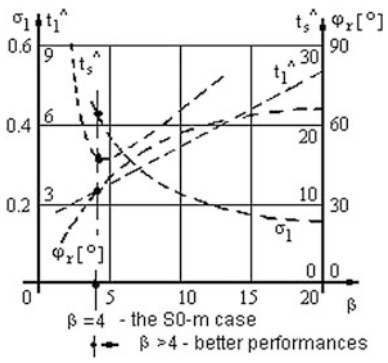

Fig. 30.3 Performance indices, σ_1, $\hat{t}_s = t_s/T_\Sigma$, $\hat{t}_1 = t_1/T_\Sigma$ and ϕ_r [°] versus β

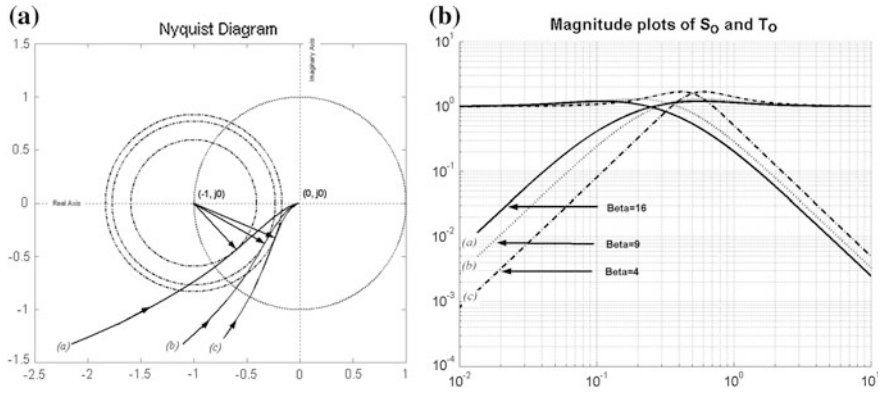

Fig. 30.4 **a** Nyquist curves and M_{S0}^{-1} *circles*, **b** Magnitude plot of the $M_P(\omega)$ for $\beta = 4, 9, 16$

- *Magnitude plot of the complementary sensitivity function*, $T_0(s)$; the dependences are depicted in Fig. 30.4b, having the characteristic values $M_{p\max(\beta=4)} \approx 1.6823$, $M_{p\max(\beta=9)} \approx 1.2990$ and $M_{p\max(\beta=16)} \approx 1.1978$.

The method offers good support to controller design for plants with variable input and continuously variable parameters, for example, variation of k_P in a relatively large domain $[k_{P\min}, k_{P\max}]$ or/and T_1 (the greatest time constant) the possibility for online (re)computing the controller's parameters (accepting an adequate value of β, which ensures a minimum guaranteed phase margin [6]. This situation is imposed by electrical drives with variable moment of inertia (VMI) treated in Sect. 30.4.

30.3.2 The Double Parameterization of the SO-m (2p-SO-m)

The double parameterization of SO-m, referred to as 2p-SO-m [9, 10], is dedicated mainly to driving systems (speed control) characterized by the t.f.s in the forms MO-2 and MO-3 given in Table 30.3, without an integral component, having $T_1 \gg (T_2 > T_\Sigma)$ which characterize plants with variable parameters, for example driving systems with VMI. The method is based on the optimization conditions (30.3.1) using an additional parameter m defined as

$$m = T_\Sigma / T_1 \; (T_\Sigma / T_1 \ll 1). \tag{30.3.4}$$

The parameter m is a measure of the magnitude of the large time constant T_1 that points out mainly the moment of inertia. Accepting the controller-plant combination given in Table 30.3, and applying the indicated pole-zero cancelation, the t.f. computations lead to

Table 30.3 The basic situations (see also Table 30.1)

Case	$H_p(s)$	$H_c(s)$
0	1	2
2p-SO-m-1 and MO-2.1	$\frac{k_p}{(1+sT_\Sigma)(1+sT_1)}$	$\frac{k_c}{s}(1+sT_c)\,,\quad T_c=T_1$
2p-SO-m-2 and MO-3.1	$\frac{k_p}{(1+sT_\Sigma)(1+sT_1)(1+sT_2)}$ $T_1>T_2>T_\Sigma$	$\frac{k_c}{s}(1+sT_c)\frac{(1+sT_c')}{(1+sT_f)}$ $T_c'=T_2;\quad (T_c'/T_f'\approx 10)$ $\frac{k_c}{s}(1+sT_c)(1+sT_c')\,,\ T_c'=T_2$
2p-SO-m-3 (not detailed)	$\frac{k_p}{(1+sT_\Sigma)(1+sT_1)(1+sT_2)(1+sT_3)}$ $T_1>T_2>T_3>T_\Sigma,\quad T_\Sigma/T_1<0.2$	$\frac{k_c}{s}(1+sT_c)\frac{(1+sT_c')(1+sT_d)}{(1+sT_f')(1+sT_f)}$ $T_c'=T_2;\quad (T_c'/T_f'\approx 10)$ $T_d=T_3;\quad (T_d/T_f\approx 10)$

$$L(s)=H_c(s)\,H_p(s)=\frac{k_ck_p(1+sT_c)}{s(1+sT_1)(1+sT_\Sigma)},\ H_r(s)=\frac{L(s)}{1+L(s)}, \tag{30.3.5}$$

$$H_r(s)=\frac{k_ck_p+sk_ck_pT_c}{k_ck_p+s(1+k_ck_pT_c)+s^2(T_1+T_\Sigma)+s^3T_1T_\Sigma}, \tag{30.3.6}$$

(a proportional-derivative with lags (PDL-3)), having the coefficients a_ν, b_μ:

$$\begin{aligned} &a_0=k_ck_p,\quad a_1=1+k_ck_pT_c,\quad a_2=T_1+T_\Sigma,\quad a_3=T_1T_\Sigma\\ &b_0=k_ck_p,\quad b_1=k_ck_pT_c. \end{aligned} \tag{30.3.7}$$

The condition (30.3.1) is imposed in relation with the notation (30.3.4). The main situations for interest are characterized by values of $m<(\ll)1$. The substitution of (30.3.7) in the second parameterization (30.3.4) yields

$$\beta^{1/2}k_ck_p(T_1+T_\Sigma)=(1+k_ck_pT_c)^2\ \ (a)\ \ \beta^{1/2}(1+k_ck_pT_c)\,T_1T_\Sigma=(T_1+T_\Sigma)^2\ \ (b). \tag{30.3.8}$$

Finally, the characteristic t.f.s $H_0(s)$ and $H_r(s)$ will obtain the optimized forms

$$H_{0\,\mathrm{opt}}(s)=\frac{1+\beta T_{\Sigma m}s}{\beta^{3/2}T_\Sigma'\frac{m}{(1+m)^2}s(1+sT_1)(1+sT_\Sigma)}\ \text{with}\ T_\Sigma'=\frac{T_\Sigma}{(1+m)}, \tag{30.3.9}$$

$$H_{r\,\mathrm{opt}}(s)=\frac{(1+\beta T_{\Sigma m}s)}{\beta^{3/2}T_{\Sigma}^{'3}s^3+\beta^{3/2}T_{\Sigma}^{'2}s^2+\beta T_{\Sigma}^{'}s+1}=\frac{(1+\beta T_{\Sigma m}s)}{(1+\beta^{1/2}T_{\Sigma}^{'}s)[1+(\beta-\beta^{1/2})T_{\Sigma}^{'}s+\beta T_{\Sigma}^{'2}s^2]}. \tag{30.3.10}$$

The compact tuning equations are

$$k_c=\frac{(1+m)^2}{\beta^{3/2}k_pT_1\frac{T_{\Sigma}}{T_1}m}\ (1+m),\ T_c=\beta T_{\Sigma}\frac{[1+(2-\beta^{1/2})m+m^2]}{(1+m)^3}\ \text{or}\ T_c=\beta T_{\Sigma m}. \tag{30.3.11}$$

A. Performance analysis in time domain. The main system performances in time-domain regarding the reference input are synthesized in Fig. 30.5a, b. Elaborated useful conclusions are given in [10].

Values for the performance indices regarding a step disturbance are synthesized in Table 30.4. Mainly, the 2p-SO-m ensures efficient disturbance–rejection for a special case of servo system applications with "great and variable" moment of inertia.

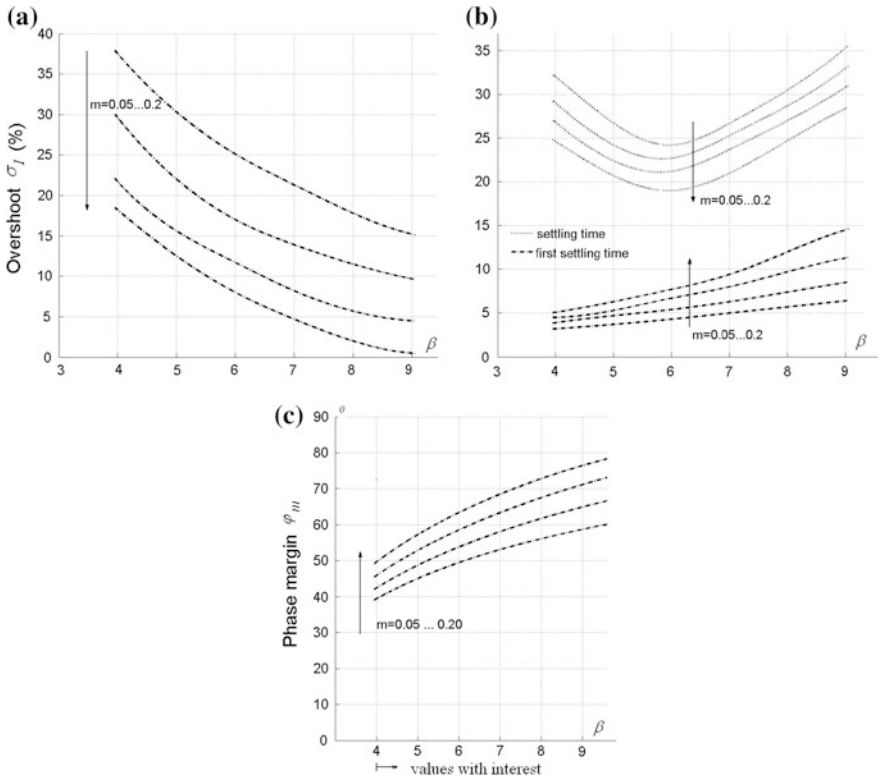

Fig. 30.5 System performance regarding the reference input; $\sigma_{1,r}, t_{s,r}, t_{1,r}=f(\beta)$, and the phase-margin curves, with m—parameter

Table 30.4 Comparison of performance indices for a step-form load disturbance

			2p-SO-m The value of β					
m		MO-m	*4*	*5*	*6*	*7*	*8*	*9*
0.05	$\hat{t}_{s,d2}$	***45,5***	**9.2**	**11.1**	**13.0**	**14.9**	**17.5**	**19.8**
	$\sigma_{1,d2}$	***9.3***	**7.7**	**8.7**	**9.7**	10.5	11.4	12.3
0.10	$\hat{t}_{s,d2}$	***28.7***	**10.6**	**12.6**	**14.5**	**17.1**	**19.6**	**23.4**
	$\sigma_{1,d2}$	***15.7***	**15.3**	17.4	19.1	20.8	22.1	2352
0.15	$\hat{t}_{s,d2}$	***19.7***	**15.2***	**17.9***	**13.9**	**16.7**	**19.7**	22.7
	$\sigma_{1,d2}$	***21.3***	22.9	25.4	28.3	30.1	32.1	34.0
0.20	$\hat{t}_{s,d2}$	***17.6***	**17.6***	**13.1**	**16.1**	19.5	22.4	26.8
	$\sigma_{1,d2}$	***25.9***	29.7	32.8	36.1	38.1	40.8	42.7

Using (30.3.9), the phase margin ϕ_r can be expressed as (Fig. 30.5c)

$$\phi_r = \text{arctg}(\beta T_{\Sigma m}\omega_c) - \text{arctg}(T_1\omega_c) - \text{arctg}(T_\Sigma\omega_c) + \pi/2. \tag{30.3.12}$$

The 2p-SO-m is recommended for servo systems (speed control) characterized by great differences between the large and the small time constants ($0.05 < m \leq 0.2$) and high performance imposed regarding load disturbances.

Comparing the control system performance indices to those ensured by the MO-m, using for β values in the of domain of $4 < \beta \leq 9$, the effects of load disturbances are lower maximum values faster rejection as shown in Table 30.4.

The 2p-SO-m is easily applicable to an analytic redesign of the controller, ensuring the "on-line" recalculation of the controller parameters, based on crisp relations.

B. Performance analysis in frequency domain. Using m and β as parameters, the Bode diagrams are illustrated in Fig. 30.6.

- ***Sensitivity function analysis***. The calculated maximum sensitivity value M_{s0} and its inverse M_{S0}^{-1} are calculated and presented only for $\beta \leq 9$ (Table 30.5).

  Remark: The dashed values are in the recommended domain or strictly close to it.

- ***Magnitude plot of the complementary sensitivity function***. For m and β as parameters, the graphics of $M_P(\omega) = |H_{ro}(j\omega)|$ are calculated and presented in Fig. 30.7 using the maximum value $M_{p\max}$ given in Table 30.6. The main conclusion, interpreted for example as in [1], is that an increased value of β leads to the decrease of the value of $M_{p\max}$ and the system becomes less and less oscillatory.

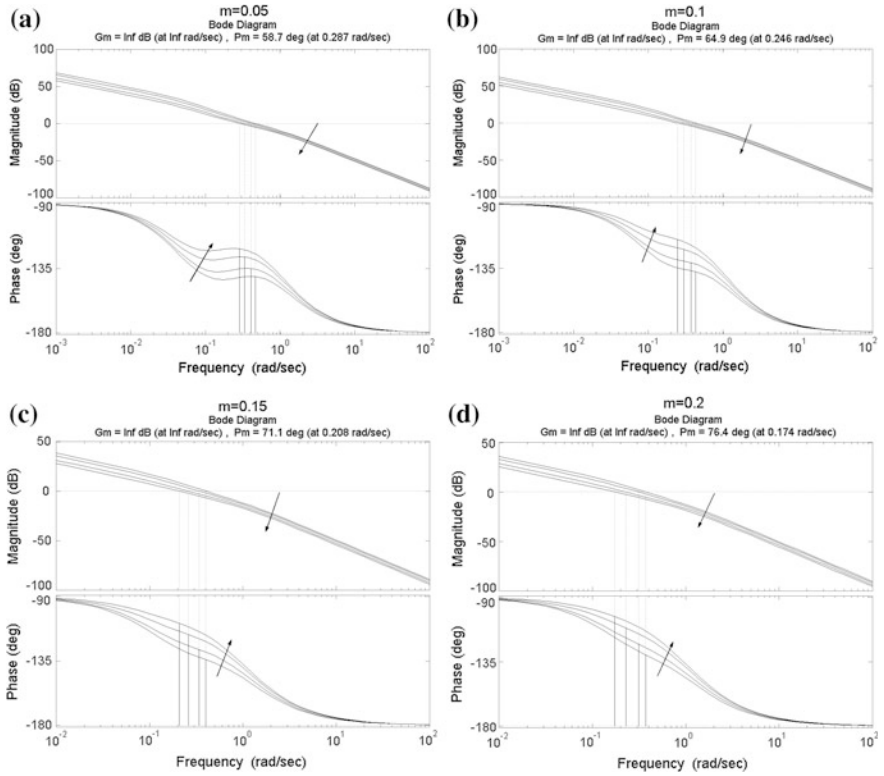

Fig. 30.6 Bode diagrams for m and β parameters

Table 30.5 The maximum value $M_{p\ max}$

	The value of β						
m	4	5	6	7	8	9	12
0.05	1.573	1.415	1.321	1.257	1.211	1.176	1.104
0.10	1.456	1.303	1.210	1.147	1.102	1.067	1.008
0.15	1.343	1.199	1.114	1.058	1.023	1.004	0.998
0.20	1.241	1.113	1.042	1.006	0.999	0.998	0.997

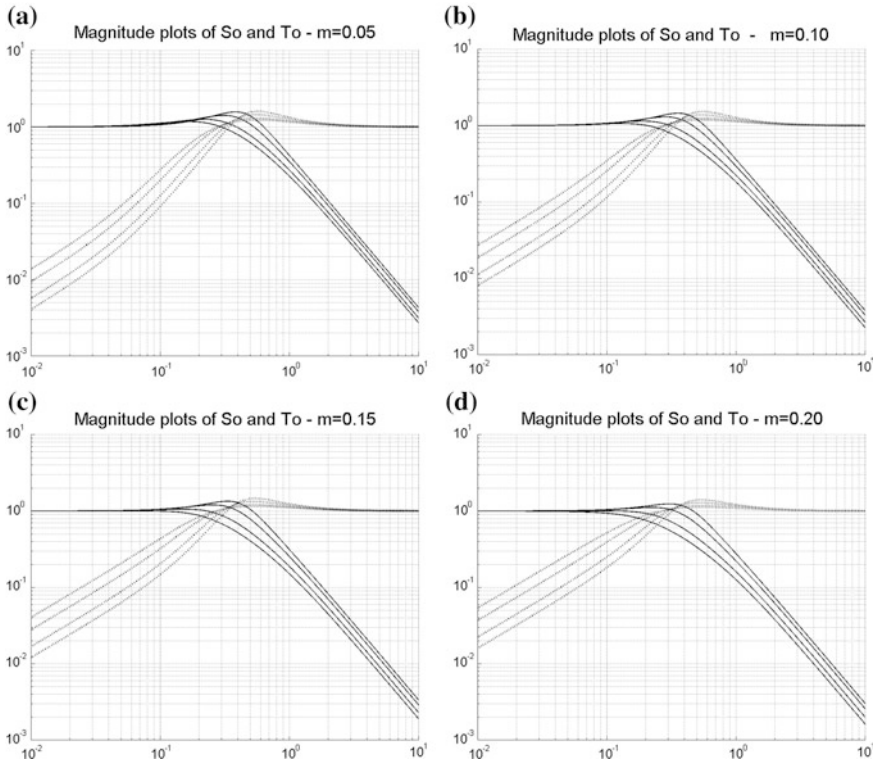

Fig. 30.7 The sensitivity and complementary sensitivity function, $\{m, \beta\}$ parameters

Table 30.6 The values for M_{s0} and M_{S0}^{-1}

		M_{s0} / M^{-1}_{s0}					
m	β	4	5	6	7	8	9
.05	M_{s0}	1.602	1.45	1.36	1.303	1.263	1.235
	M^{-1}_{s0}	**0.624**	**0.690**	**0.735**	**0.767**	**0.792**	**0.810**
.10	M_{s0}	1.529	1.385	1.302	1.248	1.212	1.185
	M^{-1}_{s0}	**0.654**	**0.722**	**0.768**	**0.801**	**0.825**	**0.844**
.15	M_{s0}	1.464	1.330	1.255	1.206	1.172	1.149
	M^{-1}_{s0}	**0.683**	**0.752**	**0.797**	**0.829**	**0.853**	**0.870**
.20	M_{s0}	1.406	1.285	1.217	1.172	1.143	1.122
	M^{-1}_{s0}	0.711	0.778	0.822	0.853	0.875	0.891

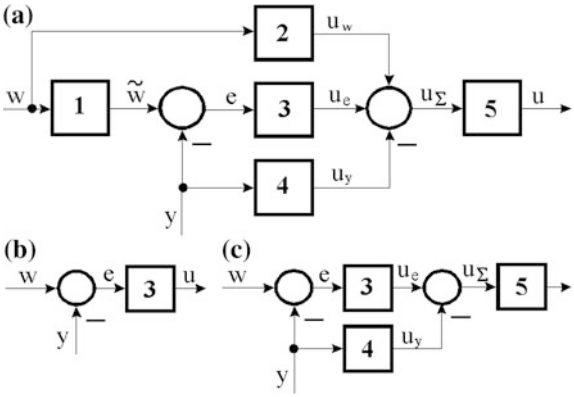

Fig. 30.8 Typical controller structures and particular forms of the modules, see for example, [19]

30.3.3 Performance Enhancement Using Reference Filters

The reference filters $F_r(s)$ are recommended for external input–output performance enhancement. The controllers with non-homogeneous structure, Fig. 30.8, for example the 2-DOF structures [18–20] are also recommended in this regard. Regarding use of reference filters, two versions are of interest:

- *A first version*, to compensate for the effect of the complex-conjugated poles in (30.3.10) and, together with this, the effect of the zero:

$$F_r(s) = \frac{1 + (\beta - \beta^{1/2})T_\Sigma s + \beta T_\Sigma^2 s^2}{(1 + \beta T_\Sigma s)(1 + sT_f s)}. \tag{30.3.13}$$

Consequently, the control system behavior in the relation $r \to r_1 \to y$ becomes aperiodical with the main performance indices $\sigma_1 = 0$ and $t_s \approx (3 \ldots 5)(\beta - 1)T_\Sigma$ (and ϕ_r according to Fig. 30.1):

$$\tilde{H}_r(s) = \frac{1}{(1 + \beta T_\Sigma s)(1 + sT_f)}. \tag{30.3.14}$$

- *A second version* of filter can be used to compensate for only the effect of the zero in (30.3.10); accordingly:

$$F_r(s) = \frac{1}{1 + \beta T_\Sigma s}. \tag{30.3.15}$$

The control system behavior in the relation $r \to r_1 \to y$ is given by the following t.f. and the closed-loop system has an oscillatory behavior only for $\beta < 9$:

$$\tilde{H}_r(s) = \frac{1}{(1+\beta^{1/2}T_\Sigma s)[1+(\beta-\beta^{1/2})T_\Sigma s+\beta T_\Sigma^2 s^2]}. \tag{30.3.16}$$

Similar types of filters are used in case of the 2p-SO-m, having the t.f.s derived from relations (30.3.5)–(30.3.9) and β and m as parameters.

30.3.4 Variable Structure for the Controller with Bumpless Switch of the Control Algorithms

The design approaches presented in previous sections are expressed in continuous time. The discretized form of the PI(D) algorithms can be obtained using, for example, the well-known classical methods [1, 2]. The discrete t.f. of the controller results in the following form exemplified for a first order controller:

$$H_C(z^{-1}) = \frac{q_0 + q_1 z^{-1}}{p_0 + p_1 z^{-1}}, \tag{30.3.17}$$

In such cases, the bumpless switching between two or more control algorithms (c.a.s) needs the re-updating of the tuning parameters.

The notations q_ν^i, $\nu = 0, 1$ are used for the coefficients of the nominator of the discrete t.f. and $i = 1 \ldots m$, and m for the number of c.a.s (here $m = 3$). If the controller operates on the basis of c.a. (1) and it switches to c.a. (2), next c.a. (2) switches to c.a. (3), the algorithms are

$$\begin{aligned} u_{mk} &= q_1^{(m)} \cdot x_{1k}^{(m)} + q_0^{(m)} \cdot x_{2k}^{(m)}, \quad m = 1, 2, 3, \quad \text{c.a.}(m) \\ \varepsilon_k^{(m)} &= \varepsilon_k, \quad \varepsilon_k = r_k - y_k \end{aligned} \tag{30.3.18}$$

$x_{1k}^{(m)} = x_{2,k-1}^{(m)}$, with values which must be calculated. Since

$$x_{2k}^{(m)} = \varepsilon_k - p_1^{(m)} \cdot x_{1k}^{(m)}, \quad m = 1, 2, 3. \tag{30.3.19}$$

Then, the c.a. (1), c.a. (2) and c.a. (3) given in (30.3.18) can be transformed into:

$$u_{mk} = q_1^{(m)} \cdot x_{1k}^{(m)} + q_0^{(m)} \cdot \varepsilon_k - q_0^{(m)} \cdot p_1^{(m)} \cdot x_{1k}^{(m)}. \tag{30.3.20}$$

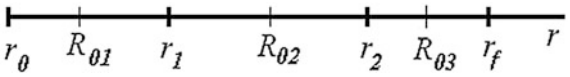

Fig. 30.9 Detailed block diagram regarded as the c.a.s switch

Imposing the bumpless switching condition $u_{2k} = u_{1k}$ and next $u_{3k} = u_{2k,}$ leads to

$$\begin{aligned} x_{1k\,\mathrm{nec}}^{(n+1)} &= (q_1^{(n)} x_{1k}^{(n)} + q_0^{(n)} x_{2k}^{(n)}) / (q_1^{(n+1)} - q_0^{(n+1)} p_1^{(n+1)}) \\ &\quad - \left[q_0^{(n+1)} / (q_1^{(n+1)} - q_0^{(n+1)} p_1^{(n+1)}) \right] \varepsilon_k, \\ x_{2,k-1\,\mathrm{nec}}^{(n+1)} &= x_{1k\,\mathrm{nec}}^{(n+1)}, \quad n = 1, 2. \end{aligned} \tag{30.3.21}$$

The switching conditions must be connected and correlated to the changes in the plant, according to Fig. 30.9 and Eq. (30.3.21) considered in relation with the switching program

$$\begin{aligned} &\text{IF } (r < r_1) \text{ THEN c.a.}(1) \\ &\text{ELSE IF } (r < r_2) \text{ THEN c.a.}(2), \\ &\text{ELSE c.a.}(3), \end{aligned} \tag{30.3.22}$$

where r is the variable parameter which imposes the switch condition, r_1, r_2, r_3 are the switching values (included in the switching conditions) r_0—the initial value and r_f—the final value of r and R_{01}, R_{02}, R_{03} are the values for which the controllers are developed.

The block diagram of the controller is given in Fig. 30.10.

30.3.5 The Automatic Tuning/Retuning Steps

Imposing the requirements regarding variable reference tracking, load disturbance, rejection and robustness (also a minimum phase margin) and plant parameter changes (m is recalculated), the area of usable of the extended design methods and the value for the parameter β and can be adopted adequately.

In the field of electric drives, where demanding requirements are often met, the procedure for a systematic tuning/retuning of PI(D) controller parameters has to solve three issues:

(1) For choosing the tuning procedure it is necessary to end up in a control loop which achieves robust performance in terms of reference tracking and output disturbance rejection.
(2) Decide the optimal PI(D) type controller for the controlled plant; decide whether the controlled process needs I, PI, or PID control; if the D part has to

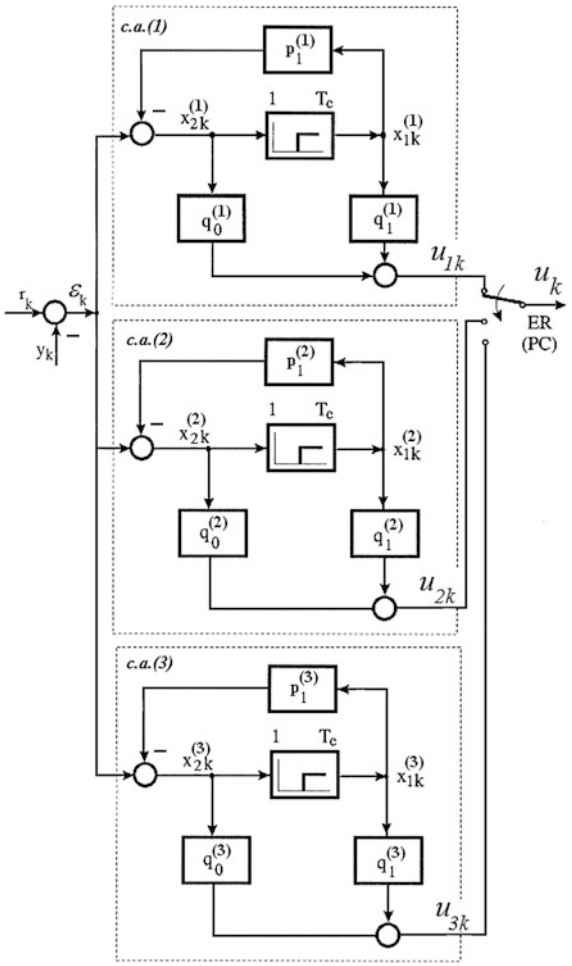

Fig. 30.10 Detailed block diagram of controller switching

be added only in the "feed-back" part of the algorithm, a non-homogenous structure results.

(3) Find the most important disturbances in the plant (external and/or parametric) and determine the effect in plant-parameter values (measured or estimated). Define an analytic form of parameter-changing.

(4) Impose the switch conditions, retune the controller's parameters based on the new model of the process and ensure a bumpless switching algorithm.

Due to the variations of the plant parameters, modifications in the controllers occur. Therefore, the method can be considered as adaptive, and the adaptive controller should have the benefit of taking into account such variations and retune its parameters.

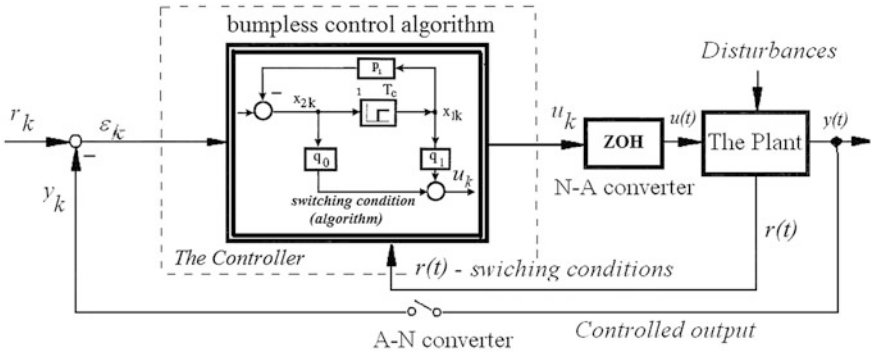

Fig. 30.11 Block diagram of control system with PI controller with bumpless switching between two or more control algorithms

If it is necessary, a stability analysis test can be applied for adjacent domains (worst cases analysis) using Kharitonov's method for a linear approach or Liapunov's method for a nonlinear approach. The switching structure presented in Fig. 30.9 and in Fig. 30.11 is applicable without difficulties to the classical (PI) case or to other derived structures. Illustrative examples are a Takagi–Sugeno PI type fuzzy controller, 2-DOF controllers, etc. [20–22].

30.4 Application: Control Structure for Mechatronic System with Variable Parameters

The essential objectives of some mechatronic applications is to ensure good reference signal tracking with small settling time with zero or small overshoot, good load (external) disturbance rejection, and reduced sensitivity with regard to parameter (internal) changes in a given domain and heavy operating regimes [15, 23–26].

Taking into account these objectives, the presented design methods ES0-m and 2p-SO-m—and based on it—different modern control solutions can be recommended and successfully applied; for example, "robust control algorithms" having the parameters permanently adapted to the variation of the plant parameters and load disturbances, adaptive fuzzy controllers (Takagi–Sugeno type), adaptive sliding-mode controllers, etc. Mainly such algorithms are based on the analytical or estimated model of the plant functioning in continuously variable conditions.

A classical application refers to electric drive systems with continuously variable reference, moment of inertia and load disturbance (abbrev. C-VR-MI-LD) for which, the variability of the parameters depends on the evolution of the plant. Representative cases are the driving systems (particularly electrical drive) with

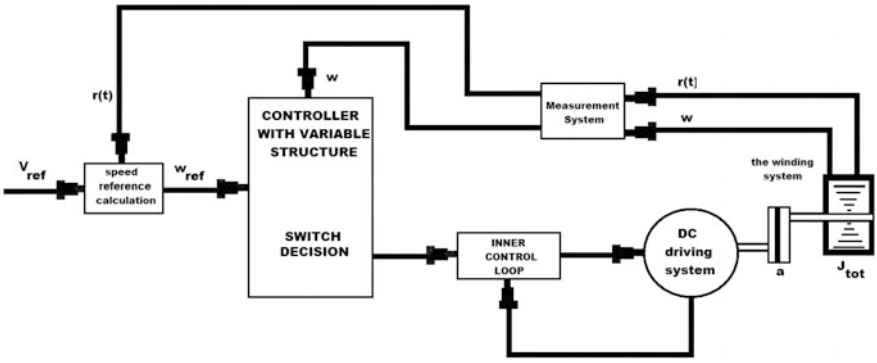

Fig. 30.12 The cascade control structure

DC-motors or BLDC-motors, [27–33] that wrap strip of various alloys on a drum (strip winding) as shown in Sect. 30.4.2.

The winding of the strip leads to the variation of the drum radius and thus the variation of the moment of inertia, which obviously changes the plant parameters and the overall system behaviors.

The speed control for the drive can be achieved using a cascade control structure (abbrev. CCS), used in the inner loop classical control solutions [27] and in the external loop PI(D) controllers (or controllers derived from it) with adaptable parameters. The functional structure of the CCS is illustrated in Fig. 30.12.

30.4.1 Steady-State Conditions and Anti-Windup Reset Measure

The mathematical model (MM) of a BLDC-m in the symmetrical operating mode [27–30] is very close to the MM of the DC-m; this leads to some similarities of the control solutions and of their design. The main (external) control loop design can be based on linearized equivalent second- or third-order benchmark-type t.f.s—see the plant t.f.s $P(s)$ in Tables 30.1, 30.2 and 30.3—connected to the operating points. So, the application became a classical control design case, with permanently adapted controller parameter based on crisp relations, see Sect. 30.3.

Table 30.7 Steady-state values of output and of control error for different values q_0

$r(s)$	y_∞			ε_∞		
	$q_0 = 0$	$q_0 = 1$	$q_0 = 2$	$q_0 = 0$	$q_0 = 1$	$q_0 = 2$
$\frac{1}{s} r_\infty$	$\frac{k_0}{1+k_0} r_\infty$	$1 \cdot r_\infty$	$1 \cdot r_\infty$	$\frac{1}{1+k_0} r_\infty$	$0 \cdot r_\infty$	$0 \cdot r_\infty$
$\frac{1}{s^2} r_\infty$	∞	∞	∞	∞	$\frac{1}{k0} r_\infty$	$0 \cdot r_\infty$

The first case, related to the ESO-m, is applied to processes with the t.f.s $P(s)$ characterized by an integral component (benchmark-type, Table 30.2).

The second case refers to speed control applications for processes with the t.f.s $P(s)$ without integral components (Table 30.3, the 2p-SO-m case), for which the condition $T_1 \gg 4T_\Sigma$ concerning the plant's t.f. is fulfilled [31].

The third case corresponds to time-variable reference input speed control structures (CS), where the applications require small control errors and so, the presence of a second integral component in the controller t.f. and, finally, in $H_0(s)$, $q_0 = 2$ in Table 30.7 is necessary (q_0 is the number of integral components). The subscript ∞ associated to a certain variable, points out the steady-state value of that variable, y and ε_∞ are the steady-state value of controlled output y and of control error ε.

In the first two cases an 1-DOF PI(D) controller can be used. The extension of the controller with an additional integral component, Fig. 30.13 is recommended only in the third case. Therefore, the controller can be characterized as an I+PI(D) with L structure and an anti-windup-reset (AWR) measure is recommended and pointed out in Fig. 30.13.

30.4.2 *Application: The Strip Winding System with Variable Moment of Inertia. Bench-Mark Type Model for Controller Design*

The C-VR-MI-LD application refers to a DC-m (it can also be a BLDC-m) [27–32], with a short (rigid) coupling with a rolling drum, which wraps a strip with thickness h and density ρ. The functional diagram of the application is presented in Fig. 30.14, where: a—the transmission parameter which characterizes the speed reduction unit, ω_f—the angular velocity (rolling drum) [rad/s], v_T—the linear velocity (rolling drum) [m/s], J_m, J_T—the moment of inertia of the DC-m and of the (rolling) drum [kgm^2], $J_{tot}(t)$—the moment of inertia of the whole system, [kgm^2], $r(t)$—the drum radius with strip wrapped on it [m], and f_h—the resistance force of the strip [N].

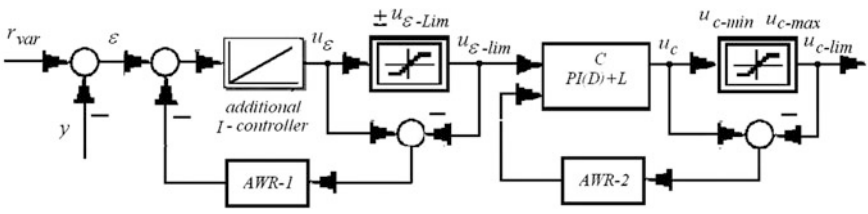

Fig. 30.13 Double integrating PI(D) controller structure with double AWR measure

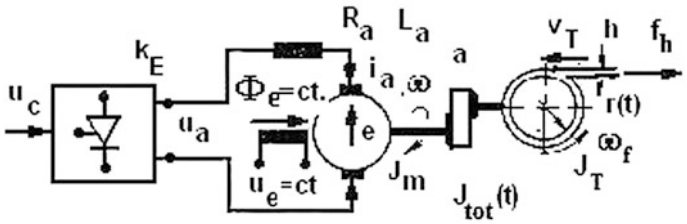

Fig. 30.14 The functional diagram of a DC electric drive system with VMI

The variation of the angular velocity of the drum and the total inertia of the system can be described by

$$\begin{aligned} a &= \omega_f / \omega, \\ J_{\text{tot}}(t) &= J_m + a^2 \cdot J_T(t). \end{aligned} \tag{30.4.3}$$

If h is sufficiently small, the drum radius variation and the variation of the moment of inertia of the drum can be approximated as (l—the drum width):

$$\begin{aligned} \frac{\mathrm{d}r(t)}{\mathrm{d}t} &= \frac{h}{2 \cdot \pi} \cdot \omega_f(t) = \frac{h}{2 \cdot \pi} \cdot a \cdot \omega(t), \\ J_T(t) &= \rho \cdot \pi \cdot l \cdot r^4(t)/2. \end{aligned} \tag{30.4.4}$$

This leads to the following extended MM of the electric drive system with VMI:

$$\begin{aligned} \frac{\mathrm{d}f_h(t)}{\mathrm{d}t} &= C \cdot a \cdot r(t) \cdot \omega(t) - C \cdot v_T(t), \\ \frac{\mathrm{d}\,i_a(t)}{\mathrm{d}t} &= -\frac{R_a}{T_a} \cdot i_a(t) - \frac{k_e}{L_a} \cdot \omega(t) + \frac{k_E}{L_a} \cdot u_c(t), \\ \frac{\mathrm{d}\omega(t)}{\mathrm{d}t} &= \frac{k_m}{J_{\text{tot}}(t)} \cdot i_a(t) - \frac{1}{J_{\text{tot}}(t)} \cdot \left[\frac{\mathrm{d}J_{\text{tot}}(t)}{\mathrm{d}t}\right] \cdot \omega(t) - \frac{a \cdot r(t)}{J_{\text{tot}}(t)} \cdot f_h(t) - \frac{k_f}{J_{\text{tot}}(t)} \cdot \omega(t), \end{aligned} \tag{30.4.5}$$

where C is the elasticity constant of the strip material. Using Eq. (30.4.3), Fig. 30.15 describes the variation of the moment of inertia (J) and also the variation of the mechanical time constant (T_m) versus drum radius (r).

Overall, the model is nonlinear considering the change of the system parameters, due mainly to changes in the moment of inertia of the drum (J_T). Accepting a constant value for the resistance force of the strip, f_h, the linear velocity (rolling drum) has an imposed constant value:

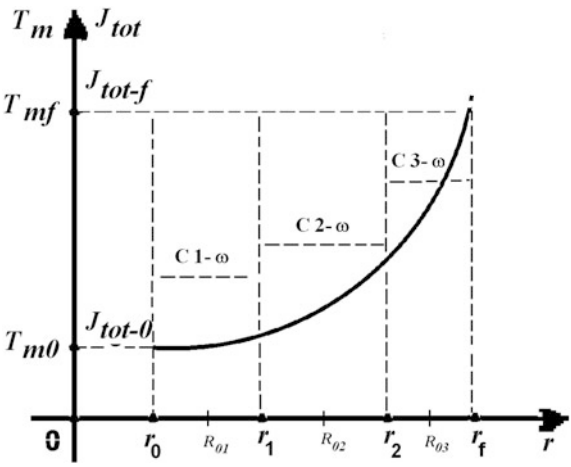

Fig. 30.15 The inertia and mechanical time constant variation as function of drum radius

$$v_T(t) \cong \text{const}, f_h(t) = \text{const} \tag{30.4.6}$$

Accepting some simplifying assumptions and using the classical linearization technique connected to fixed value of radius, simplified benchmark-type MMs outlined in Tables 30.1, 30.2 and 30.3 can be obtained. They will be used in the CS design. The online retuning of the controller parameters is connected to three fixed value of radius for which the parameters of the three digital controllers are calculated using the ESO-method, with $\beta = 9$ (ensuring the phase margin φ_r around 55°).

The simulation block diagram given in Fig. 30.16 is developed on the basis of Eqs. (30.4.3)–(30.4.6). Other solutions can employ Takagi–Sugeno PI-Fuzzy Controllers (TS-PI-FCs) speed controllers C1-ω, C2-ω and C3-ω [32]; the solution can ensure good control system performance and compensation for plant nonlinearities. The implementation of the bumpless switching PI control algorithm (c.a.) follows the steps presented in Sect. 30.3.4 assisted by Eqs. (30.3.18)–(30.3.22).

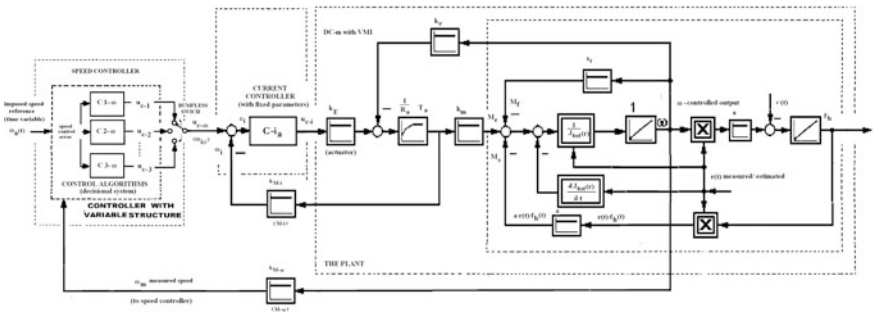

Fig. 30.16 Cascade control structure for C-VR-MI-LD driving system with a switching logic for a speed controller

30.4.3 Application: The Case Study and Simulation Results

This section offers simulation results for two possible CCS versions, which use a classical PI inner controller with fixed parameters calculated using the MO-m [1].

In the first version the speed controller comprises three digital PI controllers with fixed values for the parameters calculated relative to three significant values of the total moment of inertia reduced to the electric motor shaft, $J_{\text{tot}}(t)$: $J_{\text{tot},R01}$, $J_{\text{tot},R02}$, $J_{\text{tot},R03}$, regarding three linearization points of the radius, $R_{01} = 0.0175$ m, $R_{02} = 0.0315$ m and $R_{03} = 0.05$ m and with bumpless switching of the control signal, Fig. 30.16.

In the second version, the CCS contains only one PI speed controller with fixed parameter values designed relative to three mentioned values of the total moment of inertia. The variants are summarized in Table 30.8.

- The first version of CCS. In design step the ESO-method was applied; using a sampling time $T_e = T_{a/4} = 0.00025$ s. The parameters of the digital c.a.s are:

$$\begin{aligned} &C - i_a\text{: } q_{0i} = 1.55, \quad q_{1i} = -1.47, p_{0i} = 1, p_{1i} = -1, \\ &C_{R_{01}} - \omega\text{: } q_0^{(R_{01})} = 0.0492, \quad q_1^{(R_{01})} = -0.0483, p_0^{(R_{01})} = 1, p_1^{(R_{01})} = -1, \\ &C_{R_{02}} - \omega\text{: } q_0^{(R_{02})} = 0.134, \quad q_1^{(R_{02})} = -0.132, p_0^{(R_{02})} = 1, p_1^{(R_{02})} = -1, \\ &C_{R_{03}} - \omega\text{: } q_0^{(R_{03})} = 0.15, \quad q_1^{(R_{03})} = -0.149, p_0^{(R_{03})} = 1, p_1^{(R_{03})} = -1. \end{aligned} \tag{30.4.7}$$

Imposing a constant value for the linear velocity v_f and recalculating permanently the reference speed $\omega_0(r(t))$, the simulation results are presented in Fig. 30.17. Based on these results it can be concluded that a PI speed controller with variable parameter values and bumpless transfer of the control ensure good control performances relating to the changes of the parameters over time. Since the application has continuously variable parameters, a sensitivity analysis in frequency domain conclusions can be useful.

Table 30.8 Combinations of plant parameters and controller parameters

		R_{01}/J_{01}	R_{02}/J_{02}	R_{03}/J_{03}
L1	*C-ω Optimal for* R_{01}	*Case study 1.1* $R_{01}, C_{R01} - \omega$	*Case study 1.2* R_{02}, $C_{R01} - \omega$	*Case study 1.3* R_{03}, $C_{R01} - \omega$
L2	*C-ω Optimal for* R_{02}	*Case study 2.1* $R_{01}, C_{R02} - \omega$	*Case study 2.2* R_{02}, $C_{R02} - \omega$	*Case study 2.3* R_{03}, $C_{R02} - \omega$
L3	*C-ω Optimal for* R_{03}	*Case study 3.1* $R_{01}, C_{R03} - \omega$	*Case study 3.2* R_{02}, $C_{R03} - \omega$	*Case study 3.3* R_{03}, $C_{R03} - \omega$

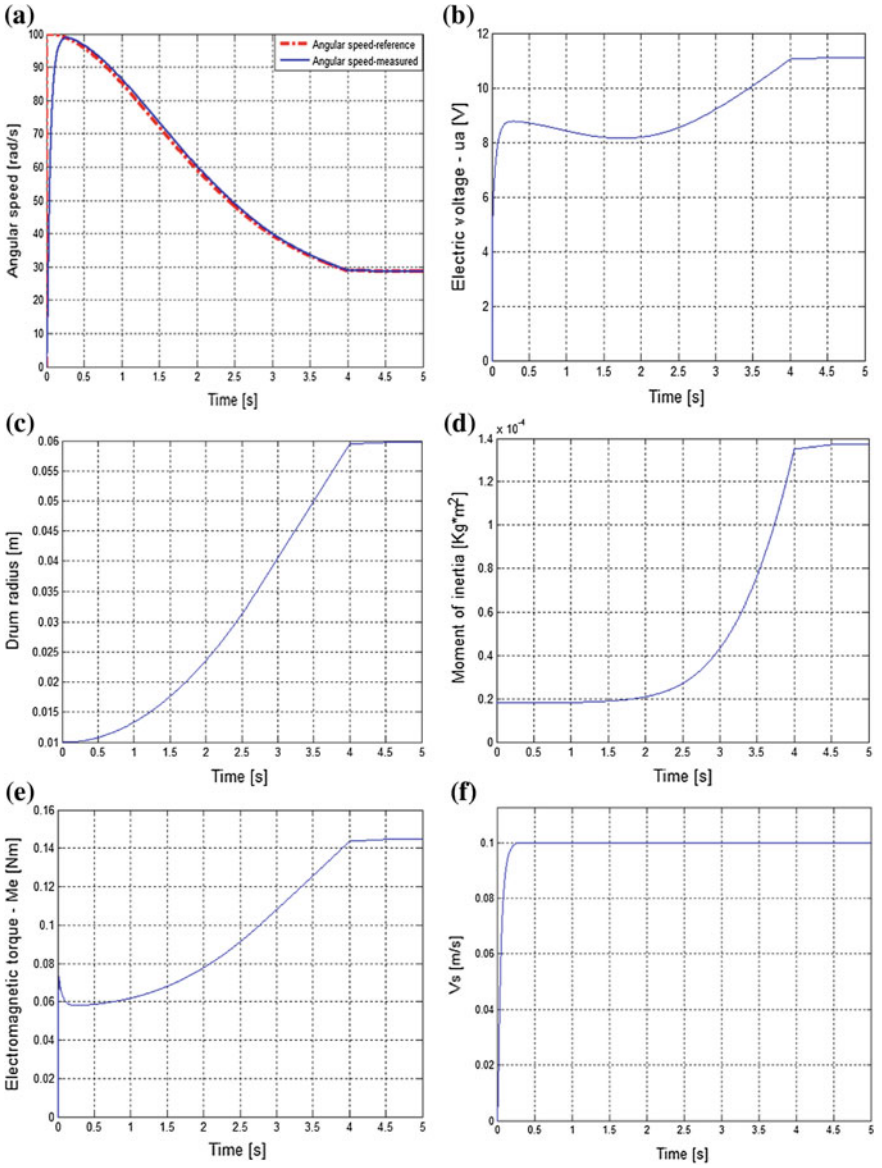

Fig. 30.17 Simulation results for C-VR-MI-LD driving system-first version of CCS: angular speed versus time (reference and measured) for the DC drive system: (**a**), electric voltage versus time for the DC drive system with VMI (**b**), drum radius versus time for the DC drive system with VMI (**c**), moment of inertia for the DC drive system with VMI (**d**), electromagnetic torque versus time for the DC drive system with VMI (**e**), linear speed of the drum versus time for the DC drive system with VMI (**f**)

- The second version of CCS. The parameters of the PI speed controllers were calculated using the ESO-m [6] ($\beta = 9$) for the same values of the radius resulting the same values of the digital c.a.s (30.4.7). In order to compare the performance of various controller-process combinations, summarized in Table 30.8 the commonly used descriptors were used: (a) step response of the angular speed versus time; (b) Bode characteristics; Fig. 30.18 presents only results for the CCS with PI current controller for the L2 and L3 combinations in Table 30.8 (*C-ω Optimal for* R_{02}, *C-ω Optimal for* R_{03}). According to [32] good performances are provided by case studies 2.1–2.3 with optimal case 2.2 and case studies 3.1–3.3 with optimal case 3.3 because in terms of settling times, $C_{R02} - \omega$ is favorable for R_{02} and least favorable for R_{01}, R_{03} and $C_{R03} - \omega$ is favorable for R_{03} and least favorable for R_{01}, R_{02}. The results are characterized by the following performance indices:

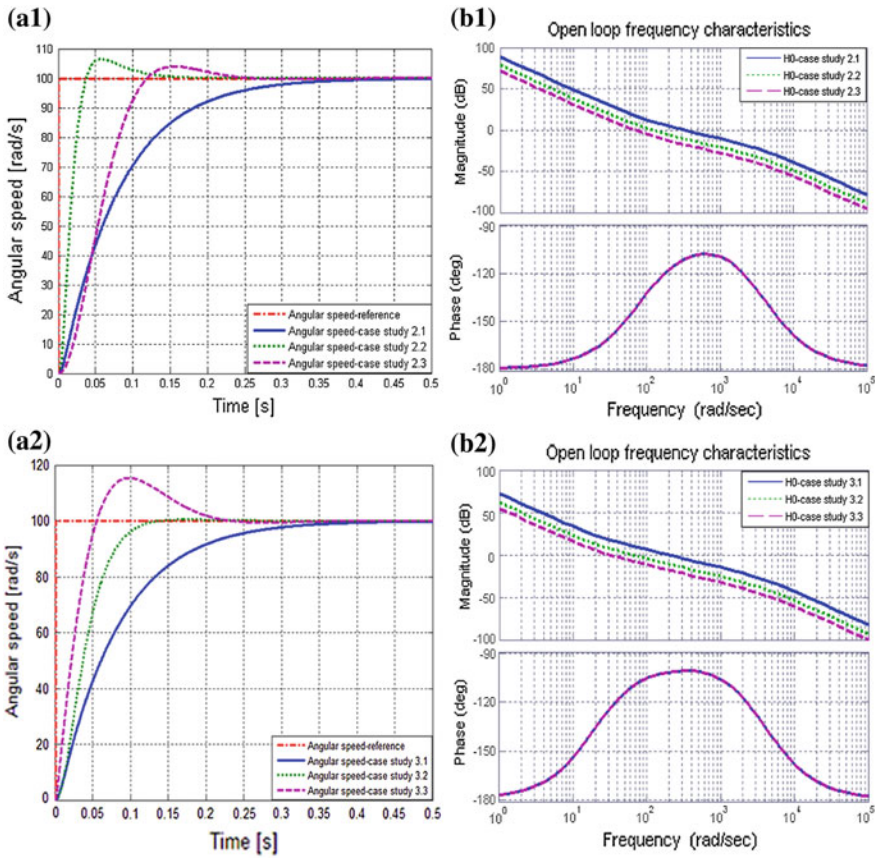

Fig. 30.18 Simulation results for C-VR-MI-LD driving system-second version of CCS: **a** step response of the angular speed versus time; **b** Bode characteristics

- *Case study 1.1*: the cutting frequency $\omega_t = 141$ rad/s, the phase margin $\varphi_r = 60°$, resonance peak $M_r = 1.28$ dB, bandwidth $\Lambda_b = 198$ rad/s and resonant frequency $\omega_r = 117$ rad/s.
- *Case study 1.2*: the cutting frequency $\omega_t = 60$ rad/s, the phase margin $\varphi_r = 39°$, resonance peak $M_r = 4.17$ dB, bandwidth $\Lambda_b = 90$ rad/s and resonant frequency $\omega_r = 55$ rad/s.
- *Case study 1.3*: the cutting frequency $\omega_t = 37$ rad/s, the phase margin $\varphi_r = 27°$, resonance peak $M_r = 7.1$ dB, bandwidth $\Lambda_b = 56$ rad/s and resonant frequency $\omega_r = 35$ rad/s.
- ***Case study 2.1***: the cutting frequency $\omega_t = 337$ rad/s, the phase margin $\varphi_r = 74°$, resonance peak $M_r = 0.0214$ dB, bandwidth $\Lambda_b = 431$ rad/s and resonant frequency $\omega_r = 225$ rad/s.
- ***Case study 2.2***: $\omega_t = 117$ rad/s, $\varphi_r = 61°$, $M_r = 1.4$ dB, $\Lambda_b = 161$ rad/s and $\omega_r = 90$ rad/s.
- ***Case study 2.3***: the cutting frequency $\omega_t = 62$ rad/s, the phase margin $\varphi_r = 47°$, resonance peak $M_r = 3.59$ dB, bandwidth $\Lambda_b = 92$ rad/s and resonant frequency $\omega_r = 49$ rad/s.
- ***Case study 3.1***: the cutting frequency $\omega_t = 201$ rad/s, the phase margin $\varphi_r = 78°$, resonance peak $M_r = 1.78$ dB, bandwidth $\Lambda_b = 233$ rad/s and resonant frequency $\omega_r = 185$ rad/s.
- ***Case study 3.2***: the cutting frequency $\omega_t = 65$ rad/s, the phase margin $\varphi_r = 70°$, resonance peak $M_r = 1.4$ dB, bandwidth $\Lambda_b = 83$ rad/s and resonant frequency $\omega_r = 34$ rad/s.
- ***Case study 3.3***: $\omega_t = 58.4$ rad/s, $\varphi_r = 58°$, $M_r = 1.25$ dB, $\Lambda_b = 81$ rad/s and $\omega_r = 50$ rad/s.

The design of the conventional controllers with fixed parameters is possible in such cases by determining the variation of the operating conditions and developing the controller for an adequately justified case. The results for the second study substantiate new control solutions that ensure the possibility to avoid the worst cases and demonstrate the need for controllers with variable parameters in variable CSs.

30.5 Conclusions

The mechatronic applications with continuously variable operating conditions (for example, variable reference, variable load disturbance, and variable moment of inertia) require adjustment of the conditions in which the controller parameters must be adaptable. To ensure good control performance, recalculation of controller parameters and providing bumpless switching between more control algorithms (in our case three) are required. To recalculate the controller parameters relations should be as simple as possible but well justified. The choice of the number of algorithms and the conditions for calculating the controller parameters are problems which need to be solved by the designer.

Based on the practical version of the SO-method, the chapter presents two extensions—the ESO-m and the 2p-SO-m—focused on benchmark-type plant models, which enable generalizations of the optimization conditions and based on it, compact design relations can be given. The presented extensions enlarge significantly the areas of application and usefulness of the SO method specific for mechatronic system applications, and they ensure better control system performance. The control design is discussed in continuous time, but the results can be easily implemented in quasi-continuous digital version using, for example, the approach given in [2].

Section 30.4 has presented a typical mechatronic application dedicated to servo systems with continuously variable conditions. In particular it is the case of a DC drive system that wraps on a drum strip of various alloys. The variation of the drum radius determines the modification of the moment of inertia, which obviously changes the plant parameters and the overall system behaviors. The basic idea of process control is to maintain a constant linear velocity of the wrapped strip by changing the angular velocity of the drum. The results presented support the benefits of design methods and their application to processes with variable parameters.

Extensions of the presented methods, i.e., Takagi–Sugeno fuzzy controller extension, the nonhomogeneous variant of the controller, are possible application themes. They can be accompanied by several modeling and application-oriented approaches [33–43].

Acknowledgments This work was supported by a grant in the framework of the Partnerships in priority areas—PN II program of the Romanian National Authority for Scientific Research ANCS, CNDI - UEFISCDI, project number PN-II-PT-PCCA-2011-3.2-0732, by a grant of the Romanian National Authority for Scientific Research, CNCS - UEFISCDI, project number PN-II-ID-PCE-2011-3-0109. Also, the work was partially supported by the strategic grant POSDRU ID 77265 (2010) of the Ministry of Labor, Family and Social Protection, Romania, co-financed by the European Social Fund—Investing in People.

References

1. Åström, K.J., Hägglund, T.: PID Controllers Theory: Design and Tuning. Instrument Society of America, Research Triangle Park, NC (1995)
2. Föllinger, O.: Regelungstechnik. Elitera Verlag, Berlin (1985)
3. Kessler, C.: Das symetrische Optimum. Regelungstechnik **6**(11), 395–400 (1958)
4. Kessler, C.: Das symetrische Optimum. Regelungstechnik **6**(12), 432–436 (1958)
5. Loron, L.: Tuning of PID controllers by the non-symmetrical optimum method. Automatica **33**(1), 103–107 (1997)
6. Preitl, S., Precup, R.-E.: An extension of tuning relations after symmetrical optimum method for PI and PID controllers. Automatica **35**(10), 1731–1736 (1999)
7. Vrancic, D., Peng, Y., Strmcnik, S.: A new PID controller tuning method based on multiple integrations. Control Eng. Pract. **7**(5), 623–633 (1999)
8. Vrancic, D., Strmcnik, S., Juricic, D.: A magnitude optimum multiple integration tuning method for filtered PID controller. Automatica **37**(9), 1473–1479 (2001)

9. Preitl, Z.: Improving disturbance rejection by means of a double parameterization of the symmetrical optimum method. Sci. Bull. "Politehnica" Univ. Timisoara, Trans. Autom. Comput. Sci. **50**(64), 25–34 (2005)
10. Preitl, Z.: Model Based Design Methods for Speed Control Applications. Editura Politehnica, Timisoara, Romania (2008)
11. Vrančić, D., Strmčnik, S., Kocijan, J., de Moura Oliveira, P.B.: Improving disturbance rejection of PID controllers by means of the magnitude optimum method. ISA Trans. **49**(1), 47–56 (2010)
12. Papadopoulos, K.G., Mermikli, K., Margaris, N.I.: Optimal tuning of PID controllers for integrating processes via the symmetrical optimum criterion. In: Proceedings of 19th Mediterranean Conference on Control and Automation (MED 2012), Corfu, Greece, pp. 1289–1294 (2011)
13. Papadopoulos, K.G., Mermikli, K., Margaris, N.I.: On the automatic tuning of PID type controllers via the magnitude optimum criterion. In: Proceedings of 2012 IEEE International Conference on Industrial Technology (ICIT 2012), Athens, Greece, pp. 869–874 (2012)
14. Papadopoulos, K.G., Margaris, N.I.: Extending the symmetrical optimum criterion to the design of PID type-p control loops. J. Process Control **22**(1), 11–25 (2012)
15. Isermann, R.: Mechatronic Systems: Fundamentals. Springer, Berlin, Heidelberg, New York (2005)
16. Preitl, S., Precup, R.-E.: Cross optimization aspects concerning the extended symmetrical optimum method. Preprints of PID'00 IFAC Workshop, Terrassa, Spain, pp. 223–228 (2000)
17. Preitl, S., Precup, R.-E.: Linear and fuzzy control extensions of the symmetrical optimum method. In: Kolemisevska-Gugulovska, T., Stankovski, M.J. (eds.) Proceedings COSY 2011 of the Special International Conference on Complex Systems: Synergy of Control, Computing & Communication, Ohrid, Macedonia, 16–20 September. The ETAI Society, Skopje, MK, pp. 59–68 (2011)
18. Precup, R.-E., Preitl, S.: Development of some fuzzy controllers with non-homogenous dynamics with respect to the input channels meant for a class of systems. In: Proceedings of European Control Conference (ECC'99), Karlsruhe, Germany, paper index F56, 6 pp (1999)
19. Preitl, S., Precup, R.-E., Preitl, Z.: Control Structures and Algorithms, vols. 1 and 2. Editura Orizonturi Universitare, Timisoara, Romania (2009) (in Romanian)
20. Preitl, S., Precup, R.-E.: Development of TS fuzzy controllers with dynamics for low order benchmarks with time variable parameters. In: Proceedings of 5th International Symposium of Hungarian Researchers on Computational Intelligence, Budapest, Hungary, pp. 239–248 (2004)
21. Preitl, S., Preitl, Z., Precup, R.-E.: Low cost fuzzy controllers for classes of second-order systems. Preprints of 15th World Congress of IFAC (b'02), Barcelona, Spain, paper index 416, 6 pp (2002)
22. Precup, R.-E., Hellendoorn, H.: A survey on industrial applications of fuzzy control. Comput. Ind. **62**(3), 213–226 (2011)
23. Koch, C., Radler, O., Spröwitz, A., Ströhla, T., Zöppig, V.: Project course 'Design mechatronic systems'. In: Proceedings of IEEE International Conference on Mechatronics (ICM 2006), Budapest, Hungary, pp. 69–72 (2006)
24. Hehenberger, P., Naderer, R., Schuler, C., Zeman, K.: Conceptual design of mechatronic systems as a recurring element of innovation processes. In: Proceedings of 4th IFAC Symposium on Mechatronic Systems (MECHATRONICS 2006), Heidelberg, Germany, pp. 342–347 (2006)
25. Pabst, I.: An approach for reliability estimation and control of mechatronic systems. In: Proceedings of 4th IFAC Symposium on Mechatronic Systems (MECHATRONICS 2006), Heidelberg, Germany, pp. 831–836 (2006)
26. Su, Y., Mueller, C.: Smooth reference trajectory generation for industrial mechatronic systems under torque saturation. In: Proceedings of 4th IFAC Symposium on Mechatronic Systems (MECHATRONICS 2006), Heidelberg, Germany, pp. 896–901 (2006)

27. Boldea, I.: Advanced electric drives. Ph.D. courses. "Politehnica" Univ. Timisoara, Timisoara, Romania (2010–2011)
28. Nasar, S.A., Boldea, I.: Electric Drives. Electric Power Engineering Series, 2nd edn. CRC Press, Boca Raton (2005)
29. Yedamale, P.: Brushless DC (BLDC) Motor Fundamentals. Application Note 885, Microchip Technology Inc., Chandler, AZ (2003)
30. Baldursson, S.: BLDC motor modelling and control—A Matlab/Simulink implementation. M. Sc. Thesis, Institutionen för Energi och Miljö, Göteborg, Sweden (2005)
31. Grimble, M.J., Hearns, G.: Advanced control for hot rolling mills. In: Frank, P.-M. (ed.) Advances in Control: Highlights of ECC'99, pp. 135–170. Springer, London (1999)
32. Stînean, A.-I., Preitl, S., Precup, R.-E., Dragoş, C.-A., Petriu, E., Rădac, M.-B.: Choosing a proper control structure for a mechatronic system with variable parameters. Preprints of 2nd IFAC Workshop on Convergence of Information Technologies and Control Methods with Power Systems (ICPS'13), Cluj-Napoca, Romania, paper index 29, 6 pp (2013)
33. Škrjanc, I., Blažič, S., Matko, D.: Direct fuzzy model-reference adaptive control. Int. J. Intell. Syst. **17**(10), 943–963 (2002)
34. Baranyi, P., Tikk, D., Yam, Y., Patton, R.J.: From differential equations to PDC controller design via numerical transformation. Comput. Ind. **51**(3), 281–297 (2003)
35. Zhao, J., Dimirovski, G.M.: Quadratic stability of a class of switched nonlinear systems. IEEE Trans. Autom. Control **49**(4), 574–578 (2004)
36. Nakashima, T., Schaefer, G., Yokota, Y., Ishibuchi, H.: A weighted fuzzy classifier and its application to image processing tasks. Fuzzy Sets Syst. **158**(3), 284–294 (2007)
37. Vaščák, J.: Approaches in adaptation of fuzzy cognitive maps for navigation purposes. In: Proceedings of 8th International Symposium on Applied Machine Intelligence and Informatics (SAMI 2010), Herl'any, Slovakia, pp. 31–36 (2010)
38. Lian, J., Zhao, J., Dimirovski, G.M.: Integral sliding mode control for a class of uncertain switched nonlinear systems. Eur. J. Control **16**(1), 16–22 (2010)
39. Milojković, M., Nikolić, S., Danković, B., Antić, D., Jovanović, Z.: Modelling of dynamical systems based on almost orthogonal polynomials. Math. Comput. Modell. Dyn. Syst. **16**(2), 133–144 (2010)
40. Tikk, D., Johanyák, Z.C., Kovács, S., Wong, K.W.: Fuzzy rule interpolation and extrapolation techniques: criteria and evaluation guidelines. J. Adv. Comput. Intell. Intell. Inf. **15**(3), 254–263 (2011)
41. Angelov, P., Yager, R.: A new type of simplified fuzzy rule-based systems. Int. J. Gen Syst. **41**(2), 163–185 (2012)
42. Triharminto, H.H., Adji, T.B., Setiawan, N.A.: 3D dynamic UAV path planning for interception of moving target in cluttered environment. Int. J. Artif. Intell. **10**(S13), 154–163 (2013)
43. Wang, Y., Yang, Y., Zhao, Z.: Robust stability analysis for an enhanced ILC-based PI controller. J. Process Control **23**(2), 201–214 (2013)